Journal of Power Sources 183 (2008) 544–550

Contents lists available at ScienceDirect

Journal of Power Sources

journal homepage: www.elsevier.com/locate/jpowsour

Cube-type micro SOFC stacks using sub-millimeter tubular SOFCs

Toshio Suzuki[a,*], Yoshihiro Funahashi[b], Toshiaki Yamaguchi[a], Yoshinobu Fujishiro[a], Masanobu Awano[a]

[a] National Institute of Advanced Industrial Science and Technology (AIST), 2266-98 Anagahora Shimo-Shidami, Moriyama-ku, Nagoya 463-8560, Japan
[b] Fine Ceramics Research Association (FCRA), 2266-98 Anagahora Shimo-Shidami, Moriyama-ku, Nagoya 463-8560, Japan

ARTICLE INFO

Article history:
Received 6 March 2008
Received in revised form 8 May 2008
Accepted 8 May 2008
Available online 16 May 2008

Keywords:
SOFC
Tubular
Ceria
Anode supported
Stack
Sub-millimeter

ABSTRACT

Fabrication and characterization of tubular SOFCs under sub-millimeter (0.8 mm), bundles and stacks for low temperature operation were shown. The materials used in this study were Gd doped CeO_2 (GDC) for electrolyte, NiO–GDC for anode and (La, Sr)(Co, Fe)O_3 (LSCF)–GDC for cathode, respectively, and LSCF for supports of the tubular cells for bundle fabrication. After applying a sealing layer and current collector for each bundle of five micro tubular SOFCs, each bundle was stacked vertically, to build a four-storey cube-type stack with volume of about 0.8 cm^3. The performance of the stack was shown to be 3.6 V OCV and 2 W maximum output power under 500 °C operating temperature. Preliminary quick start-up test was also conducted at the condition of 3 min start-up time from 150 to 400 °C for 5 times, and the results showed no degradation of the performance during the test.

1. Introduction

Solid oxide fuel cells (SOFCs) have been investigated as one of the ideal energy sources from environmental issues point of view, because of high energy efficiency and fuel flexibility, and many efforts were made for the development of SOFCs [1–5]. Currently, decrease of operating temperature under 700 °C becomes one of the main research targets because it can decrease material degradation, prolong stack/module lifetime, and reduce cost by utilizing cost effective materials for stack fabrication. So far, a number of studies related to reducing SOFC operating temperature have been reported [6–18], introducing new materials and microstructures for electrolyte, cathode and anode.

On the other hand, use of small-sized tubular SOFCs may also assist further improvement of SOFCs, since it has shown high mechanical strength during rapid start-up operation [19,20] as well as high single cell performance under 600 °C operating temperature [21]. Thus, it is expected to accelerate the commercialization of SOFC systems which can be applied to portable devices, co-generation systems and auxiliary power units for automobile.

The NEDO project "Advance Ceramic Reactor" aims to develop high performance electrochemical reactors (SOFCs, for example) possibly used at low temperature with quick start-up/shut-down operation. Thus, micro tubular and honeycomb design for electrochemical reactors were selected, and the development of innovative fabrication process technology for such electrochemical reactors was mainly targeted. The goals of this project are, by 2009, (1) to develop materials for electrodes and electrolyte that can be operable at low temperature, (2) to establish manufacturing process technology that allows fabricating and integrating of micro reactors, (3) to conduct fabrication and evaluation of prototype modules. Evaluation of the prototype modules will cover wide variety of application use, such as SOFCs, hydrogen generation as well as environmental purification. In the project, thirteen research institutes, universities and companies were involved to achieve these goals, and we (AIST and FCRA) are focusing on the development of manufacturing technologies for micro integrated reactor modules for SOFC application. So far, we have developed successive manufacturing process technology for fabricating micro tubular cells with under 2 mm (Ø 2–0.8 mm) diameter and cube-type micro tubular SOFC bundles with Ø 2 mm tubular cells [22].

In this study, fabrication and characterization of the micro tubular SOFCs (Ø 0.8 mm), bundles and stacks are shown. We proposed a newly designed, cube-type SOFC stack consists of four bundles, which consist of five tubular cells (Ø 0.8 mm) and porous cathode matrices as supports of the tubular cells. The stack was designed by optimizing the property of the cathode matrix, whose gas per-

* Corresponding author. Tel.: +81 52 736 7295; fax: +81 52 736 7405.
E-mail address: toshio.suzuki@aist.go.jp (T. Suzuki).

0378-7753/$ – see front matter © 2008 Elsevier B.V. All rights reserved.
doi:10.1016/j.jpowsour.2008.05.026

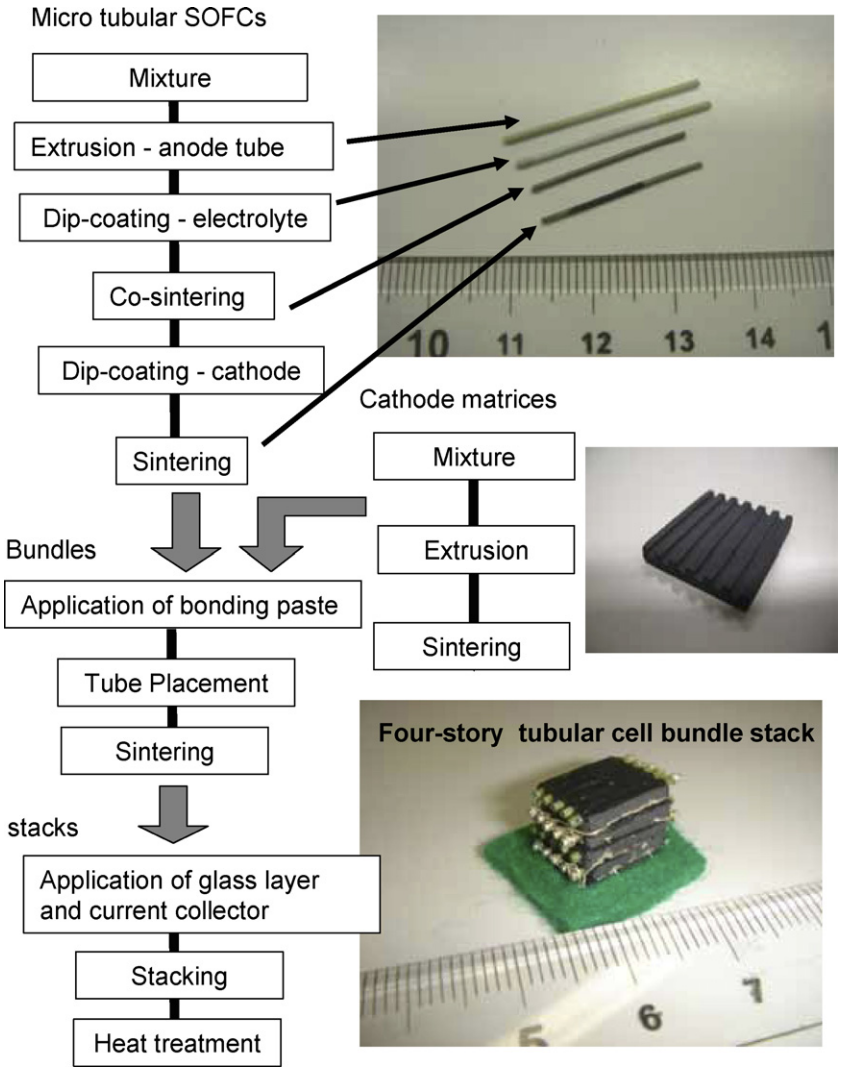

Fig. 1. Fabrication process of cube-type micro SOFC stack using sub-millimeter tubular SOFCs.

meability and electrical conductivity were previously investigated [23]. The stack performance test was conducted to seek the possibility of application of SOFCs in the temperature range under 500 °C. In addition, preliminary quick start-up test was also conducted at the condition of 3 min start-up time from 150 to 400 °C for several times.

2. Experimental

2.1. Fabrication of the micro tubular SOFC stack

Fig. 1 shows the processing procedure of the tubular SOFCs, bundle and stack. Anode tubes were made from NiO powder (Seimi Chemical Co., Ltd.), $Gd_{0.2}Ce_{0.8}O_{2-x}$ (GDC) (Shin-Etsu Chemical Co., Ltd.), poly methyl methacrylate beads (PMMA) (Sekisui Plastics Co., Ltd.), and cellulose (Yuken Kogyo Co., Ltd.). After adding a proper amount of water, these powders were mixed using a mixer 5DMV-rr (Dalton Co., Ltd.) in a vacuumed chamber. The tubes were extruded from the clay using a piston cylinder type extruder (Ishikawa-Toki Tekko-sho Co., Ltd.) with a metal mold of out Ø 1.0 mm–in Ø 0.6 mm.

An electrolyte was prepared on the surface of the anode tube by dip-coating a slurry which consists of the GDC powder used in the anode tube preparation, solvents (methyl ethyl ketone and ethanol), binder (poly vinyl butyral), dispersant (polymer of an amine system) and plasticizer (dioctyl phthalate), and co-sintered at 1400 °C for 1 h in air. Typical thickness of the electrolyte layer is around 10 μm after sintering. The diameter of the tube after sintering was 0.8 mm. A cathode was also prepared on the electrolyte by dip-coating the slurry of $La_{0.6}Sr_{0.4}Co_{0.2}Fe_{0.8}O_{3-y}$ (LSCF) powder (Seimi Chemical, Co., Ltd.), the GDC powder, and organic ingredients. Fig. 1 (left top) also shows the image of a green tube, a green tube with dip-coated electrolyte, as sintered tube with electrolyte, and a complete cell, respectively. Final dimension of the cell was Ø 0.8 mm with 0.18 mm anode wall thick.

A cathode porous structure (matrix) to bundle the tubular SOFCs was prepared using LSCF powder (Daiichi Kigenso Kagaku Kogyo Co., Ltd.), poly methyl methacrylate beads (PMMA) and cellulose (Yuken Kogyo Co., Ltd.). These powders were mixed and extruded from a metal mold using a screw cylinder type extruder (Miyazaki Tekko Co., Ltd.). The microstructure of the cathode matrices was controlled by changing the amount and diameter of the pore-former, the grain size of the starting LSCF powder and sintering temperatures.

For connecting tubular SOFCs and the cathode matrix, a bonding paste was used, prepared by mixing the LSCF powder, the binder (cellulose), the dispersant (polymer of an amine system), and the solvent (diethylene glycol monobutyl ether). The paste was painted on the surface of the cathode matrices, followed by the placement

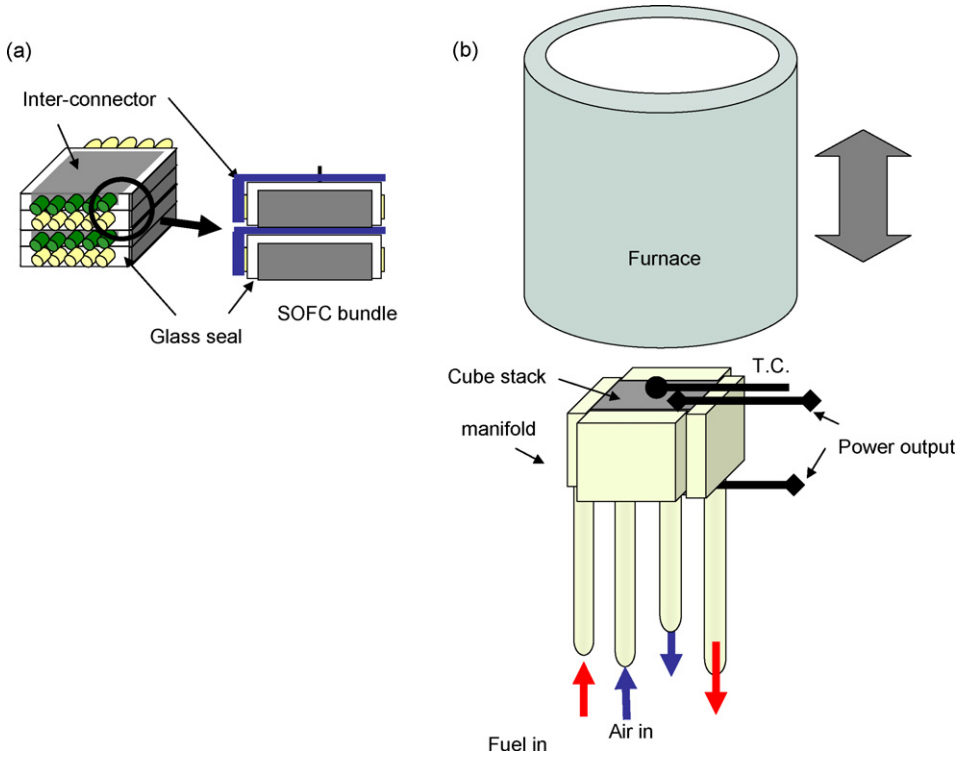

Fig. 2. (a) A schematic image of the cube-type micro SOFC stack with the volume of 0.8 cm^3 and (b) experimental setup for stack performance test.

of five tubular cells and sintered at 1000 °C for 1 h in air. Afterwards, glass seal and inter-connector (Ag sheet, wire and paste, connected to the anode of all tubes in parallel) were applied to complete the bundle as shown in Fig. 2(a). Finally, the stack was assembled by accumulating four bundles using Ag paste

2.2. Characterization of single micro tubular SOFCs and the stack

The microstructure of the anode tubes with electrolyte sintered at various temperatures was observed by using SEM (JEOL, JSM6330F). The porosity of the anode tubes and cathode matrices was measured by using mercury porosimeter (CE Instruments Co., Ltd., Pascal 440). Electrical conductivity of the anode tube and cathode matrix at operating conditions (for example, anode tube in hydrogen) was also investigated. For the estimation of gas pressure difference for air supply, gas permeability of the cathode matrix was measured. Detail was shown elsewhere [24].

The single cell performance was investigated by using a potentiostat (Solartron 1296). The cell size was 0.8 mm in diameter and 8 mm in length with cathode length of 5 mm, whose effective cell area was 0.13 cm^2. The Ag wire was used for collecting current from anode and cathode sides, which were both fixed by Ag paste. The current collection from anode side was made from an edge of the anode tube, and the collection from cathode side was made from whole cathode area. Hydrogen (humidified by bubbling water at room temperature) was flowed inside of the tubular cell at the rate of 5 mL min^{-1} + nitrogen 10 mL min^{-1}. The cathode side was open to the air without flowing gas.

Experimental set up of the stack are shown in Fig. 2(b). Gas manifolds for fuel and air for inlet and outlet were fixed to the stack with the thermocouples to monitor stack temperature and gas out let temperatures. The discharge characterization was investigated by using a Parstat 2273 (Princeton Applied Research) in DC four-point probe measurement. The Ag wire was used for collecting current from anode and cathode sides, which were both fixed by Ag paste. Hydrogen (humidified by bubbling water at room temperature) was flowed at the rate of 100 mL min^{-1} and the air was flowed at the rate of 500 mL min^{-1} at the cathode side. For the preliminary quick start-up/shut-down test of the stack, the furnace was lifted up and down to control the temperature of the stack as shown in Fig. 2(b).

3. Results and discussion

3.1. Microstructure of the anode tube (porosity) and electrolyte on the anode tube

Fig. 3 shows the porosity (before reduction) of the anode tube as a function of sintering temperature. As can be seen, Fig. 3 showed

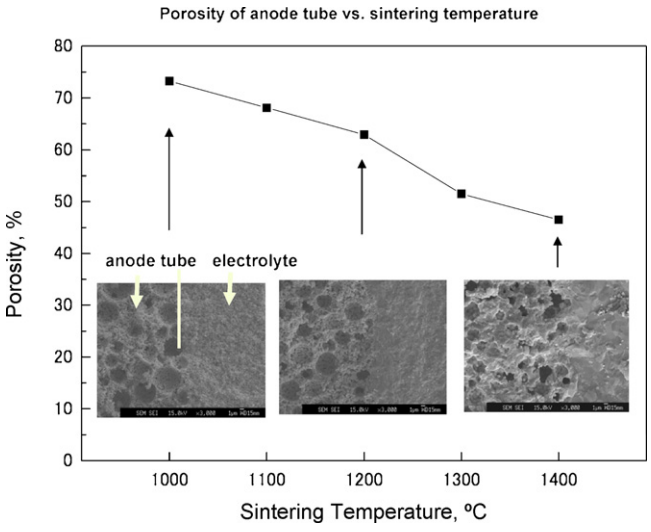

Fig. 3. Porosity of the anode tube as a function of co-sintering temperature.

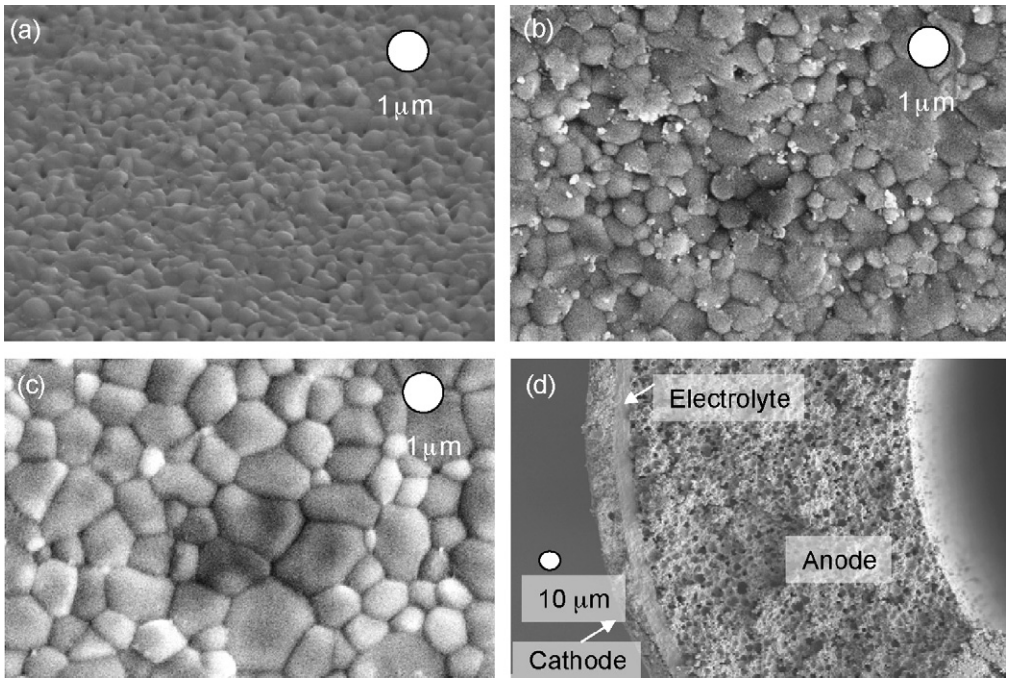

Fig. 4. SEM images of the surface of the electrolyte on the anode tube for various co-sintering temperatures: (a) sintering temperature (T_s) = 1200 °C, (b) T_s = 1300 °C, (c) T_s = 1400 °C, and (d) cross-section SEM image of Ø 0.8 mm micro tubular SOFC.

a slight change in the tendency of the porosity as a function of sintering temperature at 1300 °C, which can be correlated to the change in the size of pores in the anode tube over 1300 °C sintering temperature. After all, we have succeeded to prepare porous anode-supported tubular SOFC with 46% of porosity (before reduction). The electrical property of the anode tube was summarized in Table 1. As can be seen, the electrical conductivity of over 2000 S cm^{-1} was realized for the sample with the porosity of 46%.

Fig. 4 shows that SEM images of the electrolyte obtained at the sintering temperatures between 1200 and 1400 °C. It was observed that the microstructure of the electrolyte sintered under 1300 °C included pores in the structure and the densification of the electrolyte completed at the sintering temperatures above 1300 °C. As a result, crack-free electrolyte layer without delaminating from the anode tube was realized with controllable thickness of 10–30 μm. Note that it is also important for anode support to have sufficient shrinkage to densify the electrolyte layer, which requires at least 10% linear shrinkage [25].

3.2. Gas permeability and electrical conductivity of the cathode matrix

Table 2 shows the property of the cathode matrices prepared from 20 μm LSCF powders. We have shown that the microstrucure of the cathode matrix can be effectively controlled by changing the grain size of starting material. The porosity of the cathode matrix was 78%, corresponding to the variation of gas permeability 6.2×10^{-4} ml cm cm^{-2} s^{-1} Pa^{-1}. The electrical conductivity of the specimen was ranged from 56.2 to 57.1 S cm^{-1} at between 400 and 600 °C due to high porosity of the specimen, which were far lower than bulk conductivity over ~300 S cm^{-1} [26].

Table 1
Properties of the anode tube for the micro tubular SOFC support

Porosity (%)	46
Conductivity (S cm^{-1})	
@400 °C	2681
@500 °C	2429
@600 °C	2233

Table 2
Properties of the cathode matrix for the micro SOFC bundle

Porosity (%)	78.2
Gas permeability (ml cm cm^{-2} s^{-1} Pa^{-1})	6.2×10^{-4}
Conductivity (S cm^{-1})	
@400 °C	57.1
@500 °C	57.6
@600 °C	56.2

Fig. 5 shows the relationship between maximum gas(air) flow in the SOFC bundle (25–0.8 mm diameter micro tubular SOFCs in 1 cm^3 under given gas pressure differences using the gas permeability on Table 2. As can be seen, above 8 kPa pressure difference (room

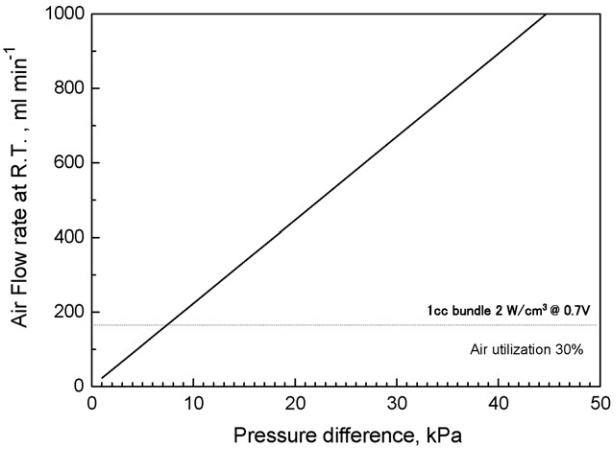

Fig. 5. Possible gas flow rate in the cathode matrix as a function of gas pressure difference.

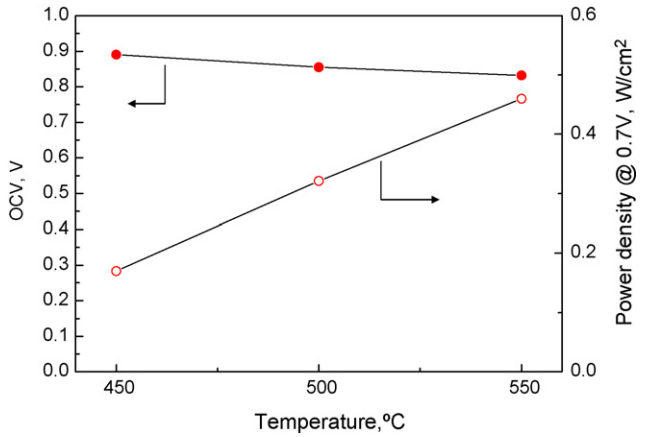

Fig. 6. Performance of the single 0.8 mm diameter tubular SOFC. OCVs and power density @ 0.7 V for operating temperatures from 450 to 550 °C.

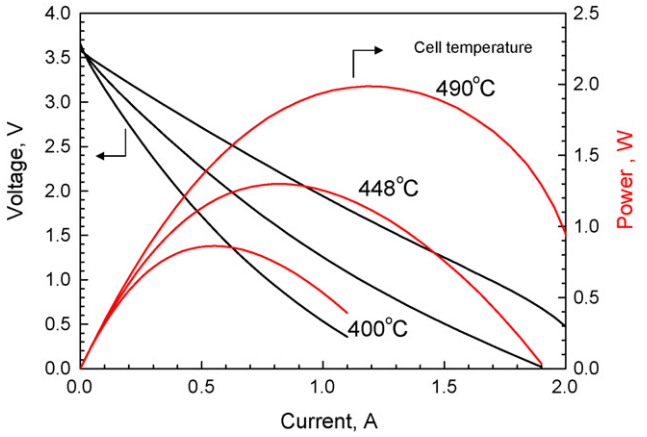

Fig. 7. Performance of the micro SOFC stack (0.8 cm^3) at the stack temperature under 500 °C.

temperature basis), it was possible to obtain sufficient gas (air) flow to achieve 2 W cm^{-3} at 0.7 V (dashed line in Fig. 5), which is our target volumetric power density, assuming that air utilization is 30%.

3.3. Performance of the single micro tubular SOFC (0.8 mm diameter)

Single cell performance test was conducted using wet H_2 fuel in the temperature range of 450–550 °C. The *I–V* characteristic and power density of the cell was estimated from the area of the cathode and was shown in Fig. 6. The peak power densities of 273, 628 and 1017 mW cm^{-2} were obtained at 450, 500, and 550 °C operating temperature, respectively. Since cell components were prepared from typical materials [27] these outstanding performances seem to be resulted from favorable anode microstructure for gas flow as well as electrochemical reaction of the fuel in the anode. The open circuit voltages were dropped from 0.89 to 0.83 V as the temperature increased from 450 to 550 °C, which was lower than theoretical OCV value of a signle cell is around 1.14 V @ 500 °C [28]. It can be said that lower OCV was resulted from the use of ceria based electrolyte [28–30], and compared to those literatures, OCV obtained for the ceria-based SOFC was a reasonalble value. An increase of electronic conductivity in ceria electrolyte during cell operation and/or direct reaction of a part of hydrogen and oxygen due to physical gas leakage through gas sealant can be reasons of this behavior. Several efforts were made to overcome this problem, such as use of an interlayer to ceria-based electrolyte to block the leak current [31–34]. On the other hand, there is a report that the leak current can be canceled out during cell operation [35]. This means that the efficiency drop due to use of ceria based electrolyte can be minimized by optimizing the operating conditions as well as the design of a SOFC system.

Since, the thickness of the tube was about 180 μm with the porosity of about 46% (before reduction), it is expected to realize light-weighted SOFC bundle/stack. The weight of single tube, bundle and stack was summarized in Table 3. As can be seen, 0.015 g per 1 cm tube length, 0.42 g per bundle including 5 tubular cells, cathode matrix (0.2 cm^3) glass seal, and current collector.

3.4. Performance of cube-type SOFC stack

Fig. 7 shows the performace of the four-storey bundle stack with the volume of 0.8 cm^3. The open circuit voltage of obtained at 400–490 °C stack temperature was 3.6 V (0.9 V per bundle), which was similar to that of single micro tubular cell. Table 4 shows the temperature of each measurement point in Fig. 2 at various stack temperatures. As can be seen, outlet gas temperaure is always higher due to reacitons inside the stack. Currently, temperature distribution and gas flow inside the cathode matrices are under investigation using simulation to optimaize the design of the stack. The output powers of 0.3, 0.44, and 2.0 W were obtained for 400, 448, and 490 °C stack tempertures, respectively, corresponding to 1, 1.6, and 2.5 W cm^{-3}. According to Table 3, about 1 W g^{-1} (per stack weight) was achieve under 500 °C operating temperature. Total electrode area of the tubular SOFCs is 5 cm^2 and thus, the power density of 0.4 W cm^{-2} was obtained at 490 °C stack temperature. Compared to the single cell performance as shown in Fig. 6 (0.32 W cm^{-2} @ 0.7 V at 500 °C), the bundle performance of the stack turned out to be 0.25 W cm^{-2} @ 0.7 V at 490 °C, which is lower than that of signle cell. This difference could be resulted from uneven temperature distribution in the stack as well as different fuel flow rate. Currenly, simulation study and improvement of fablication techonlogy for the stack are intensively focused in order to improve the stack performance.

Preliminary quick start-up test was also conducted at the condition shown in Fig. 8, 3 min start-up time from 150 to 400 °C and 9 min from 400 to 150 °C for 5 times. Runs 1, 2 and 3 represent the measurement of the stack performance at each point shown in Fig. 8. Fig. 9 shows the results of performance test obtained at 400 °C stack temperature. As can be seen, there was no obvious sign of degradation after 5 time heat cycle.

Currently, integration technology of the tubular SOFC stack is examined to obtain higher output voltage. This bundle design allows easy fabrication of stacks with any output power, and

Table 3
Weight of the tubular cell, bundle and stack, and total electrode area per stack

Tubular cell (g cm^{-1})	0.015
Bundle with glass seal (g)	0.42
0.8 cm^3 four-storey stack (g)	2.1
Total electrode area (per stack) (cm^2)	5

Table 4
Stack and gas-out temperature for *I–V* measurement of micro SOFC stack

Stack temperature (°C)	Anode out (°C)	Cathode out (°C)
400	462	440
448	528	482
490	558	527

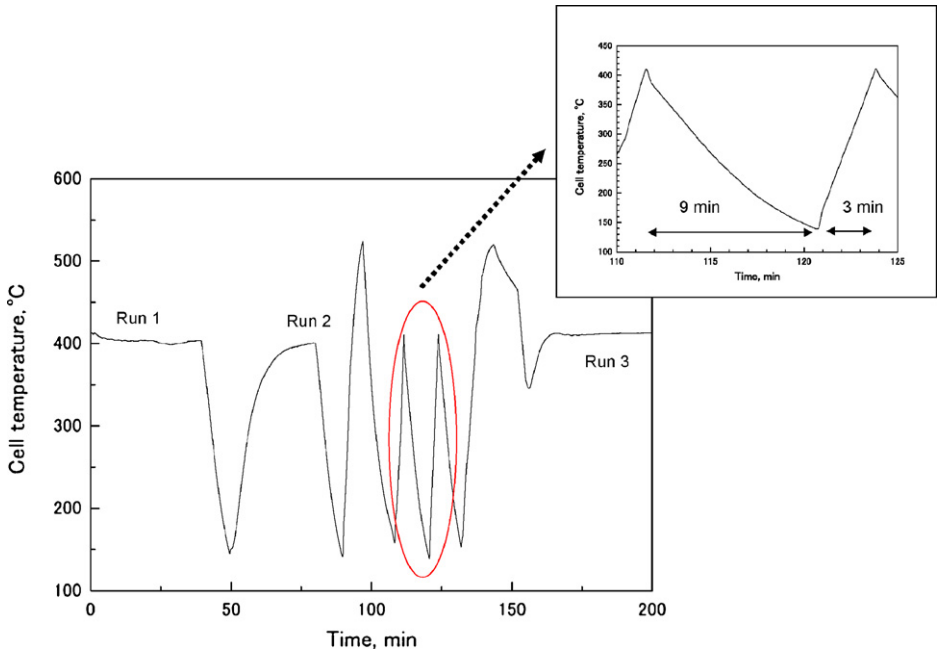

Fig. 8. Temperature load applied to the micro SOFC stack for quick start-up/shut-down test.

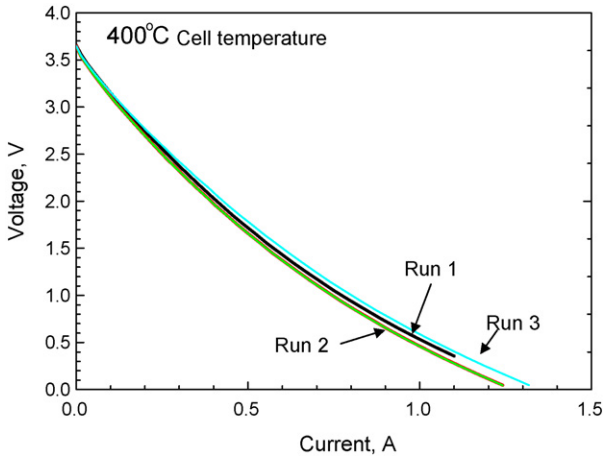

Fig. 9. *I–V* characterization of the micro SOFC stack after the temperature load shown in Fig. 8.

voltage, and therefore, use of the micro SOFC bundles for module fabriation could be ideal especially for portable SOFC systems.

4. Conclusions

A newly developed tubular SOFC stack which consists of three tubular SOFC bundles was proposed and fabricated. Fabrication and characterization of the micro tubular SOFCs (0.8 mm), bundles and stacks are shown. We proposed a newly designed, cube-type SOFC stack consists of four bundles, which consist of 5 tubular cells (0.8 mm diameter) and porous cathode matrices as supports of the tubular cells. The stack was designed by optimizing the property of the cathode matrix, whose microstructure and electrical conductivity were previously investigated. The stack performance test was conducted to seek the possibility of application of SOFCs in the temperature range under 500 °C. In addition, preliminary quick start-up test was also conducted at the condition of 3 min start-up time from 150 to 400 °C for several times, which showed stable performance during the test.

Acknowledgment

This work had been supported by NEDO, as part of the Advanced Ceramic Reactor Project.

References

[1] O. Yamamoto, Electrochim. Acta 45 (2000) 2423.
[2] N.Q. Minh, J. Am. Ceram. Soc. 78 (1993) 563.
[3] S.C. Singhal, Solid State Ionics 152–153 (2002) 405.
[4] S. de Souza, S.J. Visco, L.C. DeJohnge, J. Electrochem. Soc. 144 (1997) L35.
[5] A.V. Virkar, J. Chen, C.W. Tanner, J.W. Kim, Solid State Ionics 131 (2000) 189.
[6] B.C.H. Steele, Mater. Sci. Eng. B 13 (1992) 79.
[7] T. Ishihara, H. Matsuda, Y. Takita, Solid State Ionics 79 (1995) 147.
[8] H.G. Bohn, T. Schober, J. Am. Ceram. Soc. 83 (2000) 768.
[9] Z. Shao, S.M. Haile, Nature 431 (2004) 170–173.
[10] B.C.H. Steele, Solid State Ionics 129 (2000) 95.
[11] K. Kuroda, I. Hashimoto, K. Adachi, J. Akikusa, Y. Tamou, N. Komado, T. Ishihara, Y. Takita, Solid State Ionics 132 (2000) 199.
[12] S.P. Yoon, J. Han, S.W. Nam, T.H. Lim, I.H. Oh, S.A. Hong, Y.S. Yoo, H.C. Lim, J. Power Sources 106 (2002) 160.
[13] B.C.H. Steele, A. Heinzel, Nature 414 (2001) 345–352.
[14] S.P. Simner, J.F. Bonnett, N.F. Canfield, K.D. Meinhardt, V.L. Sprenkle, J.W. Stevenson, Electrochem. Solid State Lett. 5 (2002) A173.
[15] H. Huang, M. Nakamura, P.C. Su, R. Fasching, Y. Saito, F.B. Prinz, J. Electrochem. Soc. 154 (1) (2007) B20–B24.
[16] K. Eguchi, T. Setoguchi, T. Inoue, H. Arai, Solid State Ionics 52 (1992) 165.
[17] T. Hibino, A. Hashimoto, K. Asano, M. Yano, M. Suzuki, M. Sano, Electrochem. Solid State Lett. 5 (2002) A242.
[18] J. Yan, H. Matsumoto, M. Enoki, T. Ishihara, Electrochem. Solid-Sate Lett. 8 (8) (2005) A389–A391.
[19] K. Kendall, M. Palin, J. Power Sources 71 (1998) 268–270.
[20] K. Yashiro, N. Yamada, T. Kawada, J. Hong, A. Kaimai, Y. Nigara, J. Mizusaki, Electrochemistry 70 (12) (2002) 958–960.
[21] P. Sarkar, L. Yamarte, H. Rho, L. Johanson, Int. J. Appl. Ceram. Technol. 4 (2) (2007) 103–108.
[22] T. Suzuki, Y. Funahashi, T. Yamaguchi, Y. Fujishiro, M. Awano, J. Alloys Compd. 451 (2008) 632–635.
[23] Y. Funahashi, T. Shimamori, T. Suzuki, Y. Fujishiro, M. Awano, ECS Trans. 7 (1) (2007) 643–649.
[24] Y. Funahashi, T. Shimamori, T. Suzuki, Y. Fujishiro, M. Awano, J. Power Sources 163 (2007) 731–736.
[25] T. Yamaguchi, T. Suzuki, S. Shimizu, Y. Fujishiro, M. Awano, J. Membr. Sci. 300 (2007) 45–50.

[26] L.W. Tai, M.M. Nasrallah, H.U. Anderson, D.M. Sparlin, S.R. Sehlin, Solid State Ionics 76 (1995) 273.
[27] P. Bance, N.P. Brandon, B. Girvan, P. Holbeche, S. O'Dea, B.C.H. Steele, J. Power Sources 131 (2004) 86.
[28] Y.J. Leng, S.H. Chan, S.P. Jiang, K.A. Khor, J. Power Sources 170 (2004) 9–15.
[29] E.D. Wachsman, Solid State Ionics 152–153 (2002) 657.
[30] Y. Xiong, K. Yamaji, N. Sakai, H. Negishi, T. Horita, H. Yokokawa, J. Electrochem. Soc. 148 (2001) E489.
[31] A. Tomita, S. Teranishi, M. Nagao, T. Hibino, M. Sano, J. Electrochem. Soc. 153 (6) (2006) A956–A960.
[32] Y. Mishima, H. Mitsuyasu, M. Ohtaki, K. Eguchi, J. Electrochem. Soc. 145 (1998) 1004–1007.
[33] D. Hirabayashi, A. Tomita, T. Hibino, M. Nagao, M. Sano, Electrochem. Solid-Sate Lett. 7 (10) (2004) A318–A320.
[34] Y. Yoo, J. Power Sources 160 (2006) 202–206.
[35] R.T. Leah, N.P. Brandon, P. Aguiar, J. Power Sources 145 (2005) 336.